Carbohydrate Research 346 (2011) 1767–1775

Contents lists available at ScienceDirect

Carbohydrate Research

journal homepage: www.elsevier.com/locate/carres

Dibutylsilylene–pentose bis-chelates: on the glycoses' binding sites for strongly Lewis-acidic centres

Johanna Schulten, Peter Klüfers *

Department of Chemistry, Ludwig-Maximilians-Universität München, Butenandtstr. 5–13, D-81377 Munich, Germany

ARTICLE INFO

Article history:
Received 5 April 2011
Received in revised form 30 May 2011
Accepted 31 May 2011
Available online 2 July 2011

Keywords:
Silicon
Pentoses
Open-chain monosaccharides

ABSTRACT

Excess di(*tert*-butyl)silylene (DTBS) bis(trifluoromethanesulfonate) formed bis-DTBS derivatives with the four aldopentoses (arabinose, lyxose, ribose and xylose). The structure of the bis-chelates was affected by the bulk of the DTBS groups and the requirement of flat silacycles in the case of five-membered chelate rings. These restrictions resulted in unusual cyclic bis-chelates for ribofuranose ($\kappa O^{1,5},\kappa O^{2,3}$ bis-chelate) and lyxopyranose ($\kappa O^{1,4},\kappa O^{2,3}$ bis-chelate of a twisted boat conformation). Most importantly, all aldopentoses formed bis-chelates of their open-chain *aldehydo* isomers. The bis-chelates of *aldehydo*-arabinose and -xylose were $\kappa O^{2,3},\kappa O^{4,5}$-bonded and thus exhibited five-membered chelate rings. The bis-chelates of *aldehydo*-lyxose and -ribose were $\kappa O^{2,4},\kappa O^{3,5}$-bonded and resembled six-membered chelate rings. For lyxose, the *aldehydo* bis-chelate was isolated as a solid. The molecular structures were assigned by a combined ^{1}H, ^{13}C, and ^{29}Si NMR spectroscopic approach, which was supported by X-ray analyses on crystals of the bis-DTBS chelates of $\kappa O^{1,2},\kappa O^{3,5}$-bonded *rac*-xylofuranose, $\kappa O^{1,5},\kappa O^{2,3}$-bonded D-ribofuranose, and $\kappa O^{2,4},\kappa O^{3,5}$-bonded *aldehydo*-D-lyxose.

1. Introduction

Reducing sugars (aldoses and ketoses = 'glycoses') are configurationally labile. At equilibrium, they develop various isomers such as the α- and β-furanose as well as the α- and β-pyranose, and, to a small extent, the open-chain aldehyde and the aldehyde hydrate. Since all these isomers are interconvertible, a glycose provides, from the viewpoint of coordination chemistry, a dynamic ligand library to a central metal or semimetal.[1] As an example to illustrate this property, the reaction of the aldopentose lyxose with excess amounts of various (semi)metal probes can be examined (Chart 1). To facilitate comparison, the various bonding modes of lyxose are drawn for the L-enantiomer, regardless of whether an actual compound was described with the D-enantiomer or the racemate. Furthermore, coordination chemistry nomenclature is used throughout this work which includes the term 'chelate' for a sila cycle and the use of the κ convention to specify the chelates.[2] Ara*p*-, Lyx*a*- or Rib*f*-style abbreviations for the various glycose isomers follow the IUPAC recommendations for carbohydrate nomenclature.[3]

Hence, a larger central metal (Pd^{II} in Chart 1a) accepts both cis- and trans-vicinal diol functions to form stable chelates.[4] However, cis-vicinal chelation is generally preferred as shown for Cu^{II} that was found in a bis-bidentate bridging bis-chelate (Chart 1b).[4] Closer to the di(*tert*-butyl)silylene (DTBS) probe of this work is the phenylborylene function (Chart 1c). The central atom is much smaller here and requires a flat chelate ring which is not provided by either the cis- or the trans-vicinal diol functions of a pyranose in a chair conformation. Lyxose thus binds the borylene function through its 2,3-furanose-diol moiety. As a result, no second borylene function can be bonded despite the supply of further reagent.[5] Tridentate chelation was detected by M^{III}(tacn) probes (M = Co, Ga; tacn = 1,4,7-triazacyclononane) which enriched aqueous lyxose solutions with the species d and e. As for a and b, the β-pyranose is the chelator but chair inversion had taken place to provide the required O_3 pattern.[6] Eventually, the dinuclear Mo_2O_5 fragment enriches a bis-tridentate bridging bis-chelate of the β-lyxofuranose tetraanion as the only species.[7,8] What all these known lyxose chelators have in common is that they are derived from not-too-unstable configurations and conformations (compare the quantities of the isomers at equilibrium, given in the caption of Chart 1). The phenylboronic-acid ester (Chart 1c) best highlights the limitations of the known probes. If a strained structure of the lyxose chelate were required to achieve a bis-chelate, the bonding of the second (semi)metal fragment would not occur. Hence, there are just as few large chelate rings as strained glycose conformations such as pyranose boats. In particular, the unstable open-chain *aldehydo* isomer, which is the key intermediate in many glycose reactions, has not been observed as a ligand yet. In contrast to these coordination-chemical statements, the active centres of glycose-directed metallo enzymes have been found loaded with open-chain forms of their glycose substrate in recent work in structure biology

* Corresponding author. Fax: +49 89 2180 77407.
E-mail address: kluef@cup.uni-muenchen.de (P. Klüfers).

0008-6215/$ - see front matter © 2011 Elsevier Ltd. All rights reserved.
doi:10.1016/j.carres.2011.05.035

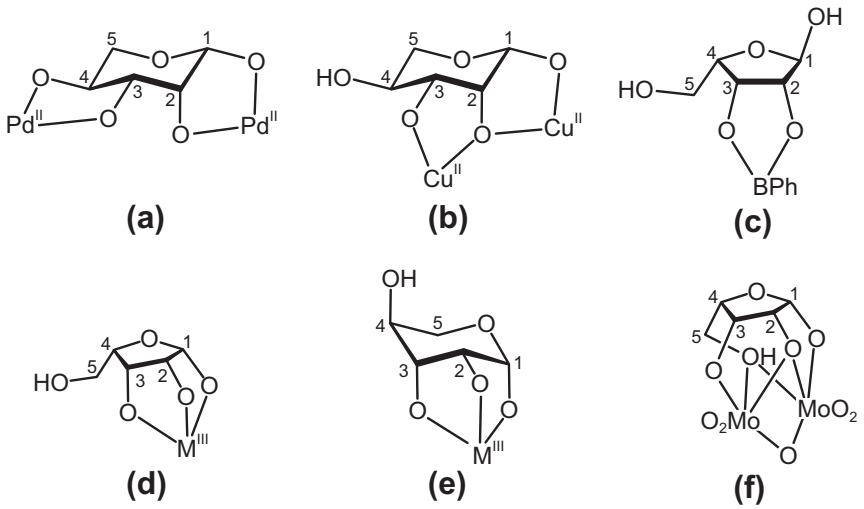

Chart 1. The products of the reaction of exhaustive quantities of various (semi)metal-probe precursors with L-lyxose; (a) Pd^{II} = Pd^{II}(en), (b) Cu^{II} = Cu^{II}(en)(H_2O) or $Cu^{II}(NH_3)_2(H_2O)$, (d, e) M^{III} = Co^{III}(tacn) or Ga^{III}(tacn); en = ethane-1,2-diamine, tacn = 1,4,7-triazacyclononane. Charges are omitted for the monocation in b and the monoanion in f.[4–8] At aqueous equilibrium, in the absence of a metal probe, the individual lyxose isomers occur in the following quantities: 71% α-pyranose, 27% β-pyranose (the isomer in a, b, and e), 1.7% α-furanose (the isomer in c), 0.6% β-furanose (the isomer in f), 0.09% aldehyde hydrate, 0.011% aldehyde (all values determined for the D-enantiomer).[9]

(glycose-related references only, without phosphates and uronates of reducing glycoses).[10–14]

Persuing the working hypothesis that stable silicon–biomolecule chelates that may occur in the course of silica biomineralisation should contain a tetracoordinate silicon central atom rather than a penta- or hexacoordinate centre, we investigated λ^4-silicon chelation by bidentately binding aldopentoses.[15] In order to probe the bidentate binding mode of the glycose, the functionality of the silicon centre was reduced to two by using the di-*tert*-butylsilylene trifluoromethanesulfonate reagent, $Si(t\mathrm{Bu})_2(OTf)_2$ ('DTBS triflate'). In glycoside chemistry, that is in the field of non-reducing sugar derivatives, DTBS triflate is used for the protection of a glycosyl donor's diol function which is remote from the anomeric centre. Examples include 3′,5′-protection of the ribofuranosyl or the arabinofuranosyl moiety as well as 4,6-protection of galactopyranosyl donors, or the protection of syn-diaxial diol functions.[16–28]

Unexpectedly, we detected bis-chelates derived from unstable configurations and conformations of the glycoses including the open-chain aldehyde. To appreciate the formation of *aldehydo*-isomer-derived chelates, some fundamentals of glycose chemistry may be recalled. The open-chain aldehyde isomers of the common aldoses are the least plentiful species in a monosaccharide's equilibrium mixture which is governed by the cyclic pyranose and furanose forms. For the four aldopentoses D-arabinose, D-lyxose, D-ribose, and D-xylose, the percentages of the aldehyde isomer have been found by NMR methods to be about 0.01, 0.01, 0.04, and 0.01, respectively (D_2O, 28 °C), roughly an order of magnitude less than the next most abundant species, the aldehyde hydrate.[9] The values are close to those obtained by a kinetic approach, the results of both investigations being fairly close to an older CD-spectroscopic determination.[29,30] The small parts of the open-chain isomers are unique to the aldoses. Glycoses of the ketose family exhibit markedly higher concentrations of the keto isomer in their aqueous equilibrium. Thus, the ketopentoses ('pentuloses') show, depending on the temperature, twenty and more percent of the open-chain keto isomer.[31,32] Even the ketohexose fructose—the related 2-epimeric aldohexoses glucose and mannose exhibiting only trace amounts of *aldehydo*-aldose (0.004%)—develops its keto form to about 3% at ambient temperature.[33–35] The small quantity of aldehyde isomer in a monosaccharide's solution equilibrium is contrasted by the significance of this isomer for the carbohydrate's chemical properties. Very basically, the interconversion reactions of the aqueous equilibrium themselves proceed through the open-chain aldehyde intermediate which is transformed to the cyclic α- and β-D-furanose and -pyranose isomers by the *si*- and *re*-attacks of O4 and O5 on the aldehyde. The fundamental significance of these reactions is underlined by the fact that they are both the subject of introductory textbooks and an area of lively research.[36,37] Attempts to expose the reactive aldehyde terminus by binding the alcoholic hydroxy functions by suitable protecting groups, require the typical multi-step procedures of carbohydrate chemistry. Examples of those attempts include the transformation of pentoses to *aldehydo*-2,3;4,5-bis(isopropylidene)pentoses via dithioacetal protection and subsequent deprotection of the aldehyde function.[38] In contrast, *keto*-fructose has recently been enriched in a simple procedure by 1-amination of this most important ketose—a fact that is, possibly, in agreement with the markedly higher percentage of the open-chain isomer at equilibrium.[39]

2. Results and discussion

2.1. Experimental strategy

The reaction of *N*,*N*-dimethylformamide (DMF) solutions of an aldopentose with the double molar amount of di-*tert*-butyl-silylene triflate proceeded under liberation of four moles of triflic acid per mole of aldose. In addition, a few reactions were performed under the standard conditions of DTBS protection which included the addition of base such as triethylamine or imidazole. In either case, general acid/base catalysis was possible and allowed the interconversion of the various aldopentose isomers despite the aprotic DMF solvent. The major aim of this work, the analysis of unusual bonding modes of glycose-derived chelators, was tackled at the stage of the reaction mixtures after 3 h of reaction time at 0 °C. The stability of the products varied markedly. Hence, some stable products could be isolated whereas unstable products decomposed on work-up. Details are given for each individual pentose. To analyse the product mixtures, standard NMR techniques were used including ^{29}Si NMR spectroscopy. The latter method turned out to be the key to limiting the number of possible products since it indicated the type of chelate formed. Hence, clearly resolved shift regions

were observed for the signals of Si atoms as part of five-membered chelate rings on the one hand, and those of six-membered rings or higher on the other. Another at-first-glance feature was provided by the ^{13}C NMR spectra. Here, the occurrence of a signal close to 200 ppm unambiguously indicated the aldehyde function of an open-chain aldopentose derivative. After the collection of such fundamental pieces of information, a detailed analysis of the pentose chelators' configuration and conformation was based on 2D NMR techniques followed by the use of an adapted Karplus relationship (see Section 4). The ^{13}C NMR part is used to illustrate the results. Figure 1 shows the assigned spectra. Each of the four aldopentoses formed an open-chain *aldehydo* derivative as a constituent of the reaction mixture. For lyxose and ribose, the depicted spectra show the distribution of the residual species in the solvent after the precipitation of most of the solid open-chain product (lyxose) or, depending on the overall concentration, some of the furanose bis-chelate (ribose). The structures of the *aldehydo* isomers were derived from ^{29}Si NMR spectra (five-ring chelates for arabinose and xylose, six-ring chelates for lyxose and ribose) and analysis of the $^{3}J_{H,H}$ coupling constants. It should be noted at this point that the established chelating mode of the DTBS protecting group is a six-membered sila cycle.[16]

What the other species have in common with the open-chain derivatives is the chelation of two DTBS groups. Signals of a monosilylated derivative found in the ribose spectrum (dashed signals in the ribose entry of Fig. 1) were the only exception. In order to unravel the rules of the aldopentose's DTBS chemistry, xylose, arabinose, ribose, and lyxose will be treated in that order.

2.2. Xylose

An aldehyde minor species and a single non-aldehyde major species was formed by the reaction of D-xylose with 2 equiv of DTBS triflate (Fig. 1, Chart 2). The minor aldehyde species

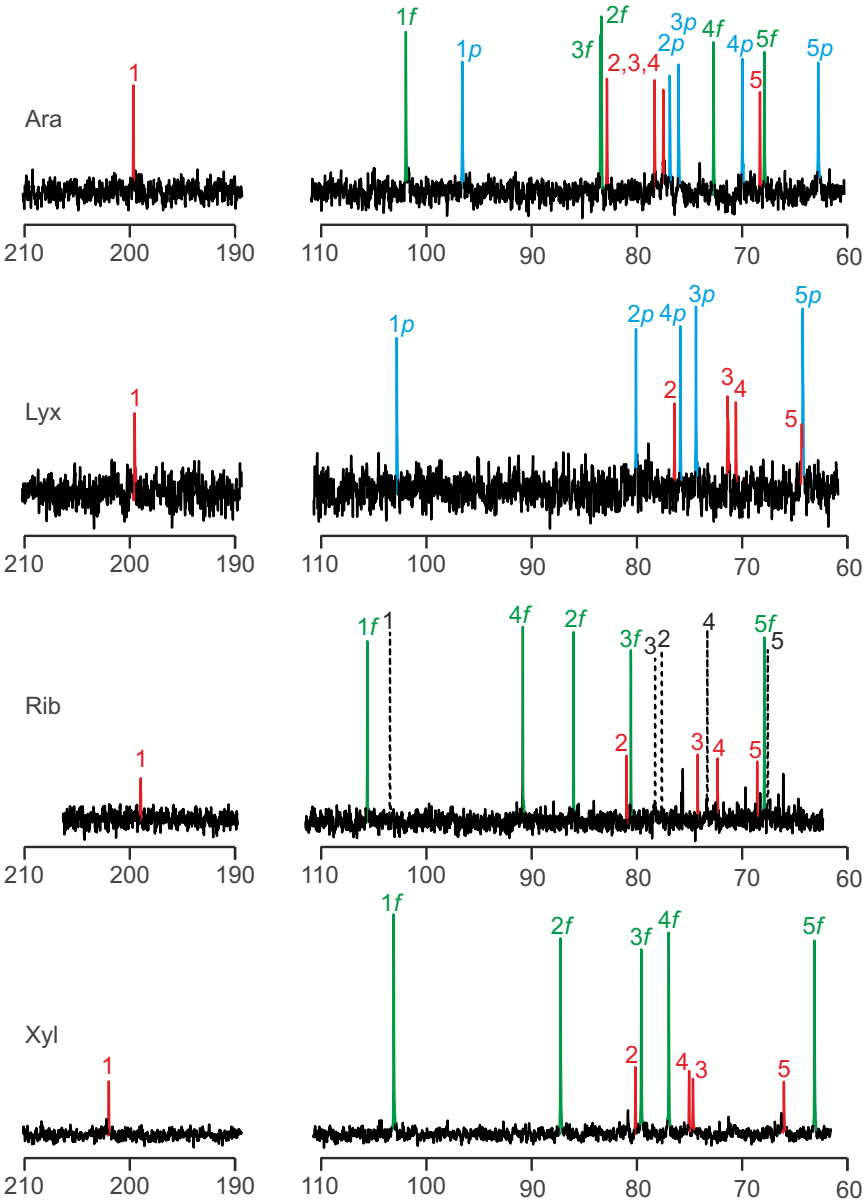

Figure 1. ^{13}C NMR spectra of the four D-aldopentoses after reaction with the double molar amount of $Si(tBu)_2(OTf)_2$ in DMF. A signal close to 200 ppm indicates an aldehyde function. For D-lyxose, the major amount of reaction product had precipitated from the DMF solution. The signal numbers refer to standard pentose numbering, *aldehydo*-pentose signals are marked by these numbers only; 'p' denotes a pyranose, 'f' denotes a furanose. The dashed signals in the ribose entry were assigned to a mono-chelate (see text).

decomposed on distilling off the solvent, whereas the major species precipitated as a crystalline solid which, after re-dissolution, resulted in the same chemical shifts in its ^{13}C NMR spectrum as found in the crude reaction mixture. The stability of the major product was checked by re-exposing the solid to triflic acid for two days at room temperature. Even then, the NMR spectra were unchanged.

For the major non-aldehyde product, ^{29}Si NMR spectroscopy indicated one five- and one six-membered chelate ring. The configurational and conformational analysis via ^{13}C and ^{1}H NMR spectroscopy revealed the α-D-xylofuranose isomer. The assignment was confirmed by the isolation of crystals whose ^{13}C NMR spectrum after re-dissolution resembled that of the major species in Figure 1 (xylose entry). However, only the principal structural features of an α-D-xylofuranose bis-chelate were resolved in the course of various attempts to analyse the crystal structure from data sets taken from the D-xylose batches. A marked disorder due to a pseudocentrosymmetric molecular arrangement prohibited reliable X-ray work. Eventually, structure analysis succeeded after using *rac*-xylose instead of the pure enantiomer to make a true centrosymmetric arrangement possible. Figure 2 shows the molecular structure of the D-enantiomer in the centrosymmetric crystals of the racemate $Si_2(t\mathrm{Bu})_4$(*rac*-Xyl*f*H$_{-4}$-κ$O^{1,2}$,κ$O^{3,5}$) (**1**). The 3,5-bonded DTBS group is in the established bonding mode described for nucleosides and arabinosides.[18,22] The other Si atom is bonded by the vicinal 1,2-diol function and is thus part of a five-membered chelate ring. The 1,2-diol torsion angle marks a relatively flat chelate ring. Assuming a limit of, say, 30° for a stable five-membered chelate ring about a tetracoordinate silicon atom, the choice for the α-xylofuranose isomer becomes clear. None of the other three isomers (α- and β-pyranose, β-furanose) provides a suitable diol function which allows for this angle at a reasonable energetic expense. The five-membered sila cycle, however, is not free of strain. The general preference of the DTBS group for six-membered chelate rings is reflected by the Si–O–C and O–Si–O bond angles.

For comparison, strain-minimised values were modelled by a computer-chemical analysis of the non-cyclic alkoxysilane di-*tert*-butyl-dimethoxy-silane at the B3LYP/6-31+G(2d,p) level of theory. The resulting values for the most stable conformer were 129.0° for the Si–O–C angles and 109.6° for the O–Si–O angle. These angles are much closer to the values within the six-membered sila cycle of **1** than to those within the five-membered ring. A final point: the preference for six-membered chelate rings by the DTBS group might have, in the case of xylose, resulted in the formation of syn-diaxial chelates (κ$O^{1,3}$,κ$O^{2,4}$) which are accessible by the inversion of the pyranose anomers' $^4C_1$ conformation. However, no such species, which have been described for a Pd^{II} bis-chelate, were detected for the silicon derivative.[1]

The major furanose derivative was accompanied by a minor *aldehydo* isomer. ^{29}Si NMR spectroscopy indicated two five-membered chelate rings for this isomer. The two-six-membered-ring

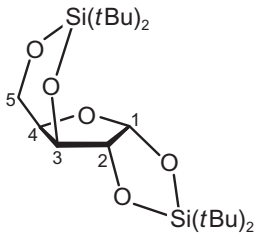

α-D-Xyl*f*H$_{-4}$-κ$O^{1,2}$,$O^{3,5}$

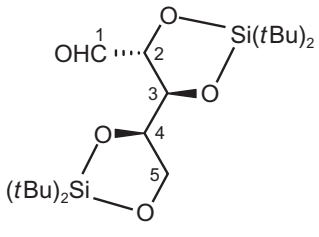

D-Xyl*a*H$_{-4}$-κ$O^{2,3}$,$O^{4,5}$

Chart 2. The products of the reaction of D-xylose and the double molar quantity of DTBS triflate in DMF.

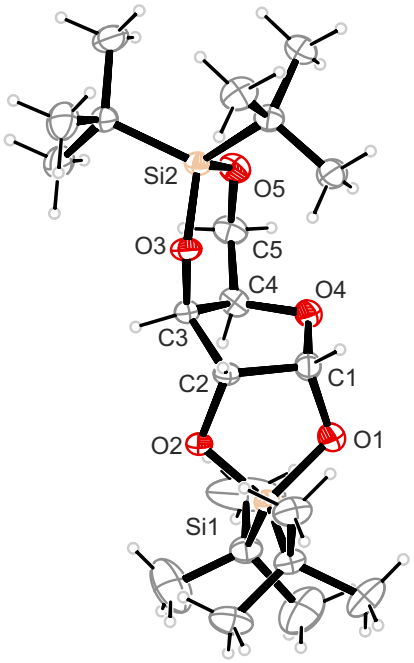

Figure 2. The D-configured isomer in crystals of **1** (add the digit '2' for atom numbering in the CIF; '1' denotes the L-isomer). Distances/Å: Si1–O1 1.662(2), Si1–O2 1.665(2), Si2–O5 1.648(2), Si2–O3 1.650(2); angles/°: O1–Si1–O2 95.7(1), O5–Si2–O3 106.5(1), C1–O1–Si1 112.9(2), C2–O2–Si1 111.6(2), C3–O3–Si2 124.4(2), C5–O5–Si2 124.4(2); O1–C1–C2–O2 −10.5(3).

alternative, which will be described in detail for xylose's 2-epimer lyxose, obviously is unstable due to the close contact of the aldehyde function and one of the DTBS groups. Moreover, the observed κ$O^{2,3}$,κ$O^{4,5}$-bonded isomer (Chart 2) shares another property with all bis-DTBS chelates of this work, namely a maximum distance of the bulky DTBS functions.

2.3. Arabinose

Arabinose formed three species of approximately equal parts on the reaction with the DTBS reagent (Fig. 1, Chart 3). The products of arabinose silylation were the least stable throughout the series of aldopentoses. Attempts to work up the reaction mixture (distilling off the solvent, re-dissolution in dichloromethane, attempted separation on silica gel) resulted in the decomposition of, first, the open-chain derivative, second, the furanose, and third, the pyranose derivative.

Despite the pronounced instability of the products, the NMR-spectroscopic analysis of the mixture was straightforward. First, an *aldehydo* isomer was enriched to a greater extent than with xylose. The ^{29}Si NMR analysis again indicated two five-membered sila cycles. As with xylose, the reason seems to be that the six-membered-ring analogue is burdened, in terms of wire models, by steric strain due to the close aldehyde–DTBS contact. By using five-membered chelate rings, a great distance between the two DTBS groups is achieved by the conformation drawn in Chart 3, which is compatible with the coupling constants. The connection of the sila cycles, however, is different for arabinose (*erythro*-connected) and xylose (*threo*-connected). If the aldehyde function is skipped, the former is a C_i-symmetric bis-chelate derived from the 2,3,4,5-erythritol part of arabinose, the latter exhibits the C_2 symmetry inherent in the 2,3,4,5-threitol partial structure of xylose.

One of the two non-aldehyde species was assigned to a furanose isomer. The NMR data for the three investigated nuclei indicated the β-D-Ara*f*H$_{-4}$-κ$O^{1,2}$,κ$O^{3,5}$ bis-chelator (Chart 3, left). It should be noted that the κ$O^{3,5}$ chelation of the DTBS function is a standard

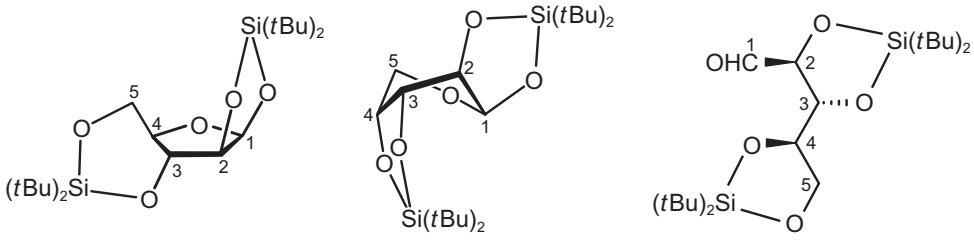

Chart 3. The products of the reaction of D-arabinose and the double molar quantity of DTBS triflate in DMF.

bonding mode used to protect arabinosides.[21,25] The other non-aldehyde species which was obviously a β-pyranose conformer due to two five-membered sila cycles (the α-pyranose would require trans-vicinal DTBS chelation which proved unsuitable for xylose), could not be assigned to a stable chair conformer in terms of $^{3}J_{H,H}$ coupling constants (the $^{1}C_{4}$ conformation would be required for double silylation; small $^{3}J_{1,2}$ and $^{3}J_{3,4}$ coupling constants and a large $^{3}J_{2,3}$ constant should have been observed then, but were not). The observed constants, however, resemble the values of the β-D-ArapH_{-4}-κ$O^{1,2}$,κ$O^{3,4}$ bis-chelator in its bis(phenylborylene) derivative. In this phenylboronic-acid diester, a twisted-boat conformation was found by X-ray crystallography.[5] The formation of a twisted boat instead of the more stable chair is caused by the smaller diol torsion angles of the former which also seems to be more suitable for the silicon compound (Chart 3, centre).

2.4. Ribose

Ribose reacted to a minor open-chain species and two major non-aldehyde derivatives (Fig. 1, Chart 4). On work-up of the mixture, the disilylated furanose derivative proved stable and was isolated as a solid.

Further minor species were visible in the spectra but not assigned. The ^{29}Si NMR signals of the *aldehydo* isomer indicated two six-membered sila cycles. The large $^{3}J_{H,H}$ coupling constants related to the chain's 2,3,4,5-part were compatible with the open-chain conformer depicted in Chart 4. The two internested six-membered chelate rings were *erythro*-linked. After the aldehyde function was removed from the open-chain bis-chelate, a C_i-symmetric fragment remained. The structural difference between the *aldehydo*-pentose bis-chelates of arabinose and xylose on the one hand and ribose on the other are correlated with the aldehyde function's binding site. For ribose, the CHO group continues the zig-zag chain of the bis-chelate in the double-six-ring structure (Chart 4), for arabinose and xylose it would not.

The spectroscopic analysis of one of the two non-aldehyde major species (dashed signals in Fig. 1) was straightforward. Both the shifts and the coupling constants were related to the standard DTBS-bonding mode of ribose, namely a κ$O^{3,5}$-bonded mono-chelate of the β-furanose isomer[18] (it should be noted that the amount of this species was not decreased in batches of a higher DTBS-triflate content). The other species's assignment, however, was bothersome. We started with an examination of ribose's possible bis-chelators. (1) In α-ribopyranose, a κ$O^{1,2}$,$O^{3,4}$-bonded bis-chelate such as the arabinopyranose boat species would bear the two bulky DTBS groups on the same side of the pyranose ring. (2) In β-ribopyranose, there would be one unsuitable trans-vicinal 1,2-chelator. (3) In α-ribofuranose, the 1,2,3-hydroxy functions of a κ$O^{1,2}$,$O^{3,5}$-bonded bis-chelate would be on the same side of the furanose ring. (4) Finally, β-Ribofuranose would provide an unsuitable trans-vicinal 1,2-diol function. The ^{29}Si NMR spectrum indicated one five- and one six-or-more-membered sila cycle. Keeping in mind an obvious preference for binding the bulky DTBS groups to diol functions on different sides of the pentose ring, the five-membered sila cycle should be formed with the 2,3-diol function. What is left for the second sila cycle, then, is a κ$O^{1,5}$ chelate which resembles a seven-membered chelate ring. The coupling constants were in agreement with this conclusion. This bonding mode of a ribofuranose molecule would have been unprecedented, however, had this assumption at that point been conclusive. Fortunately, it was this tentative species that crystallised (depending on the amount of solvent, this isomer already precipitated from the reaction batches). Figure 3 shows the result of an X-ray analysis on crystals of Si_2(tBu)$_4$(D-Rib*f*H_{-4}-κ$O^{1,5}$,κ$O^{2,3}$) (**2**). In fact, the tentative structure which was derived by the exclusion of more established alternatives, proved to be correct. In comparison to the above-mentioned angles in di-*tert*-butyl-dimethoxy-silane, the seven-membered sila cycle seems to be almost strainless in terms of C–O–Si angles but shows an enlarged O–Si–O angle, whereas the opposite holds true for the five-membered chelate ring.

2.5. Lyxose

The most unexpected result was obtained with lyxose. The formation of a dark reddish-brown reaction mixture showed partial

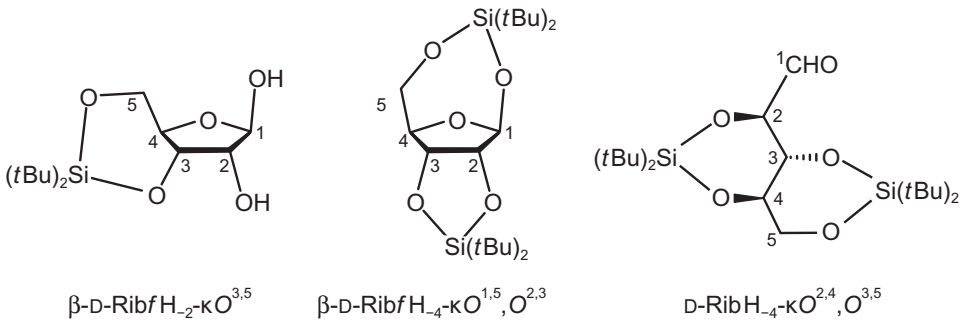

Chart 4. The products of the reaction of D-ribose and the double molar quantity of DTBS triflate in DMF.

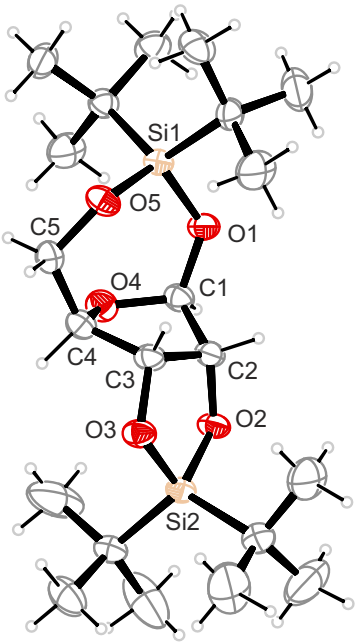

Figure 3. The molecular structure of the β-D-ribofuranose bis-chelate in crystals of **2**. Distances/Å: Si1–O5 1.647(2), Si1–O1 1.649(2), Si2–O3 1.658(2), Si2–O2 1.661(2); angles/°: O1–Si1–O5 109.4(1), O2–Si2–O3 97.1(1), C1–O1–Si1 128.0(2), C5–O5–Si1 130.1(2), C2–O2–Si2 111.3(2), C3–O3–Si2 111.2(2), O2–C2–C3–O3 20.7(3).

decomposition. Despite this fact, considerable quantities of the otherwise unisolated aldehyde isomer crystallised in the course of the reaction. The open-chain species thus formed in a markedly higher yield than the spectrum of the residual solution indicated (Fig. 1). The structure determination showed the κ$O^{2,4}$,κ$O^{3,5}$-bonded bis-chelate of *aldehydo*-lyxose (Chart 5, Fig. 4).

In solid $Si_2(tBu)_4$(D-Lyx*a*H$_{-4}$-κ$O^{2,4}$,κ$O^{3,5}$) (**3**), the C_5 backbone of open-chain D-lyxose provides two dibutylsilylene moieties with alkylenedioxy substituents in such a way that two internested sila-dioxane cycles were formed—as was derived for the ribose analogue above. In fact, lyxose shares with ribose the property that its aldehyde function continues the zig-zag chain of the 2,3,4,5-tetraol partial structure. In variance to the ribose analogue and, as with the *aldehydo*-xylose bis-chelate, skipping the aldehyde function leaves a C_2-symmetric tetraol moiety.

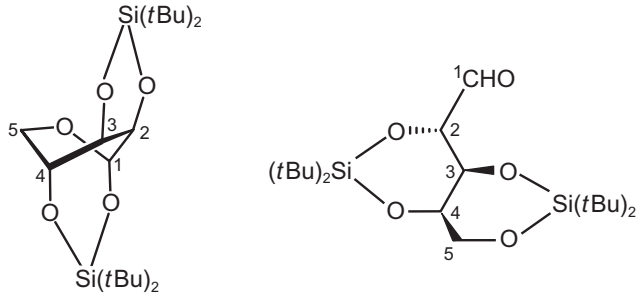

Chart 5. The products of the reaction of D-lyxose and the double molar quantity of DTBS triflate in DMF. Left: The $B_{1,4}$ conformer of the di-*tert*-butyl-silylene bis-chelate of α-D-Lyx*p*H$_{-4}$-κ$O^{1,4}$,$O^{2,3}$. Bond angles of the minimum-energy structure from DFT calculations at the B3LYP/6-31+G(2d,p) level of theory: O–Si–O: 95.1 and 106.2°, C–Si–C: 117.4 and 115.4° for the five- and the seven-membered chelate ring, respectively. Bonding angles at the O atoms: O1 127.4°, O2 112.5°, O3 112.1°, O4 128.5°. Right: the bis-silylated *aldehydo* derivative.

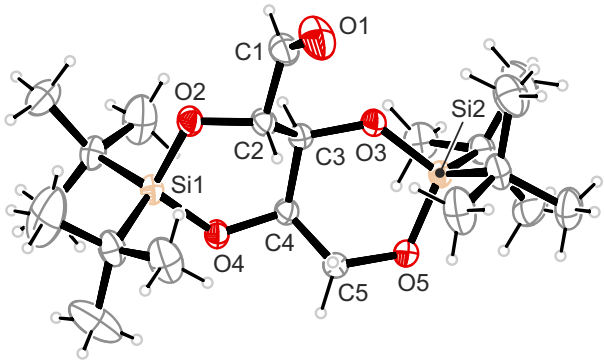

Figure 4. Molecular structure of **3** in the solvent-free crystals precipitated from a DMF solution (40% ellipsoid probability). Distances/Å: Si1–O2 1.661(1), Si1–O4 1.641(1), Si2–O3 1.640(1), Si2–O5 1.657(1), C1–O1 1.193(3); mean Si–C: 1.882 Å. Angles/°: O2–Si1–O4 105.05(7), O3–Si2–O5 105.21(7), C2–O2–Si1 118.6(1), C3–O3–Si2 128.2(1), C4–O4–Si1 128.4(1), C5–O5–Si2 118.8(1).

The decisive features of the NMR spectra, the ^{29}Si NMR chemical shifts and the $^3J_{H,H}$ coupling constants of the bis-chelate moiety, were in agreement with the solid-state result. The analysis of the major species of the residual solution (Fig. 1), was, for the same reasons, similarly intriguing as with ribose. Also with lyxose no established isomer provided a bis-chelating site in a stable conformation. With the α-furanose 1,2-trans-configured, the β-furanose would provide the bis-chelate at the same side of the furanose ring. The α-pyranose is all-trans- and the β-pyranose singly trans-configured. In the case of the related phenylboronates, lyxose (as well as ribose) resisted bis-chelate formation even at boronate-excess conditions.[5] Diol-bonding of the DTBS residue thus proved to be more compelling than that of the phenylborylene moiety. The disilylated non-aldehyde product revealed one five-membered sila cycle and one six-or-more-membered chelate ring in terms of ^{29}Si NMR spectroscopy. If great weight is given to the rule that the bulky DTBS groups must not reside in the same hemisphere about the pentose ring, again, an unprecedented bis-chelating motif resulted: the κ$O^{1,4}$,κ$O^{2,3}$-bonding boat-configured α-pyranose (Chart 5).

In order to provide more evidence for this unusual bonding mode, we chose a computer-chemical approach. The result of the structure optimisation at the B3LYP/6-31+G(2d,p) level of theory is summarised in the caption of Chart 5. In terms of the metric parameters, the usual deviations from the values of the unstrained model compound were detected. In particular, the seven-membered sila cycle is free of strain in terms of C–O–Si angles. The calculation of the ^{13}C NMR chemical shifts on the B3LYP/6-31+G(2d,p)//PBE1PBE/6-311++G(2d,p) level reproduced the measured values reliably (see Section 4).

Finally, an attempt was made to contribute to the issue of thermodynamic versus kinetic control of the reactions described in this work. We thus resubmitted isolated **3** to conditions similar to those of its formation (**3** + triflic acid in DMF) but at a lower total concentration, higher temperature (rt instead of 0 °C), and prolonged reaction time (48 h instead of 3 h). As a result, decomposition products were enriched at the expense of **3**. However, we did not succeed to characterise them.

3. Conclusion

The four aldopentoses arabinose, lyxose, ribose and xylose provide four hydroxy functions in their cyclic furanose and pyranose forms as well as in their open-chain aldehyde isomer. Probing the tetroses' bis-bidentate binding mode towards tetracoordinate silicon centres, those members of a glycose's dynamic ligand library proved to be suitable silicon chelators that resulted in a not-too-large deviation of the sila cycles' optimum metrics

(Si–O–C and O–Si–O angles). Unexpectedly, unstable glycose isomers/conformers, which have not yet been found chelating other central atoms yet, are also able to act as silicon chelators.

Due to the bulk of *tert*-butyl groups, only a few rules suffice to identify those aldopentose isomers that are capable of forming two sila cycles in the special case of DTBS binding. First, the relatively flat chelate rings require a small diol torsion angle. Considering chelation via five-membered chelate rings, this condition rules out both furanose- and pyranose-based trans-vicinal diol functions. Among the sixteen cyclic aldopentose isomers, this rule leaves β-Ara*p*, β-Ara*f*, β-Lyx*f*, α-Rib*p*, α-Rib*f*, α-Xyl*f* and β-Xyl*p* as possible chelators, the latter in its unstable all-axial $^{1}C_{4}$-D (or $^{4}C_{1}$-L) conformation. Second, a large spatial separation of the bulky dibutylsilylene functions is obviously required. This rule may be interpreted as the need for the chelating sites to reside on opposite faces of the furanose or pyranose ring. To this end, only the three stable chelators β-Ara*p*, β-Ara*f*, and α-Xyl*f*—exactly those that were found—survived. Lyxose and ribose, which could not contribute to this list, were squeezed by the DTBS reagent into bis-chelates of unprecedented structure, namely seven-membered chelate rings that required a greater (lyxose) or lesser (ribose) distortion of a stable conformation.

As the main result of this work, we detected for each of the pentoses DTBS-bis-chelates of the most important unstable glycose isomer, the open-chain aldehyde. It should be noted that the aldehyde function, which is seen as the key intermediate of many glycose reactions, is exposed in a single-step reaction here—without the established detour over the aldehyde function's pre-protection and a final deprotection step. It is worth mentioning at this point that neither a chelate of the above-mentioned all-axial β-xylopyranose isomer nor other syn-diaxial chelates were detected. This observation might not have been expected since syn-diaxial DTBS protection is among the established reactions of suitable glycosides.[24]

What stereoelectronic peculiarities of λ^4-silicon chelation can be deduced from these results that may serve as a guide to biomolecule–silicon chelation in general? The current working hypothesis focuses on the balance of Lewis acidity/basicity in the course of silicon chelation. Aldoses prefer the chelation of silicon centres by their acidic O1/O2 couple when they form bis-chelates of pentacoordinate silicates.[40] The smaller coordination number four of the silicon derivatives of this work is expected to go along with a higher Lewis acidity of the Si centre. Conversely, a stable chelate requires a higher Lewis basicity of the oxygen atoms. This requirement is matched by the anions derived from the aldose's alcoholic hydroxy functions, thus leaving the sugar's more acidic hemicacetal or aldehyde-hydrate hydroxy functions unused. The rule emerges that sufficiently strong Lewis acids probe the (generally less reactive) alcoholic hydroxy functions as the preferential sites for attack. Recalling the chelates in Chart 1, the exclusion or inclusion of a glycose's anomeric centre seems to be the decisive difference between a strong Lewis acid such as tetracoordinate silicon and weaker acidic (semi)metal centres.

4. Experimental section

4.1. Methods and materials

All starting materials were obtained from commercial sources and used without further purification. All syntheses and operations were carried out in a nitrogen atmosphere using standard Schlenk techniques. A mass spectrometer Jeol JMS 700 was used to characterise isolated products.

4.2. Crystal-structure analysis

Crystals suitable for X-ray crystallography were selected by means of a polarisation microscope, mounted on the tip of a glass fibre and investigated on a Bruker-Nonius KappaCCD diffractometer equipped with a rotating Mo anode and MONTEL-graded multilayered X-ray optics (λ = 0.71073 Å). The structures were solved by direct methods (SHELXS-97) and refined by full-matrix least-squares calculations on F^2 (SHELXL-97). Anisotropic displacement parameters were refined for all non-hydrogen atoms. Details of the analyses are collected in Table 1. CCDC 786070 (**1**), 786069 (**2**), and 763452 (**3**) contain the supplementary crystallographic data for this paper. These data can be obtained free of charge from the Cambridge Crystallographic Data Center via www.ccdc.cam.ac.uk/data_request/cif.

4.3. Computational chemistry

Structural optimisation was performed on the B3LYP/6-31+G(2d,p) level of theory with Gaussian 03.[41] For comparison with the chelates, the non-cyclic SiC_2O_2-core molecule di-*tert*-butyl-dimethoxy-silane was computed. In the most stable conformer, both methoxy functions point away from the *tert*-butyl groups. The bonding parameters are given in the text. Two less stable minimum conformers were refined whose parameters illustrate the relative softness of the bonding angles. In a C_1-symmetric conformer, one methoxy–CH_3 function points toward the *tert*-butyl hemisphere (*syn*) and the other points away from it (*anti*). Distances and angles

Table 1
Crystallographic data of **1–3**

	1	**2**	**3**
Net formula	$C_{21}H_{42}O_5Si_2$	$C_{21}H_{42}O_5Si_2$	$C_{21}H_{42}O_5Si_2$
M_r (g mol^{-1})	430.73	430.73	430.73
Crystal size (mm)	0.38 × 0.35 × 0.24	0.22 × 0.03 × 0.03	0.31 × 0.16 × 0.13
T (K)	173(2)	173(2)	200(2)
Crystal system	Monoclinic	Orthorhombic	Orthorhombic
Space group	$P2_1/c$	$P2_12_12_1$	$P2_12_12_1$
a (Å)	11.4577(2)	6.3493(1)	8.9136(1)
b (Å)	15.6307(4)	11.5295(2)	15.7204(2)
c (Å)	27.6231(7)	34.2842(7)	18.3682(2)
β (°)	92.871(1)	90	90
V/Z (Å^3)	617.61(3)	627.44(2)	643.46(1)
Z	8	4	4
ρ_{calcd} (g cm^{-3})	1.158	1.140	1.112
μ (mm^{-1})	0.170	0.167	0.163
Absorption correction	None	None	None
Reflections measured	35,914	15,569	20,407
R_{int}	0.0581	0.0585	0.0276
Mean $\sigma(I)/I$	0.0598	0.0588	0.0227
θ range	3.06–27.50	3.26–25.02	3.18–27.45
Observed refls	6530	3648	5540
x, y (weighting scheme)	0.1010, 2.7749	0.0627, 0.9758	0.0641, 0.6347
Flack parameter	—	−0.04(16)	−0.02(10)
Reflections in refinement	11,264	4443	5888
Parameters	505	253	265
Restraints	0	0	0
$R(F_{obs})$	0.0686	0.0522	0.0377
$R_w(F^2)$	0.2087	0.1302	0.1085
S	1.047	1.046	1.048
Shift/error$_{max}$	0.001	0.001	0.001
Max. electron density (e Å^{-3})	0.919	0.370	0.375
Min. electron density (e Å^{-3})	−0.483	−0.302	−0.210

are: Si–O_{syn} 1.662, Si–O_{anti} 1.655, Si–C_{mean} 1.917, C–O_{syn} 1.412, C–O_{anti} 1.417, Å; O–Si–O 104.5, C–Si–C 117.8, Si–O–C_{syn} 132.8, Si–O–C_{anti} 128.5°. In a second C_2-symmetric conformer (both methoxy–CH_3 groups *syn*, thus pointing towards the *tert*-butyl hemisphere), the molecular parameters refined to: Si–O 1.655, Si–C 1.922, C–O 1.410 Å; O–Si–O 100.3, C–Si–C 117.9, Si–O–C 133.3°.

The ^{13}C NMR shifts of the lyxopyranose compound were calculated on the B3LYP/6-31+G(2d,p)//PBE1PBE/6-311++G(2d,p) level of theory. A polarisable continuum model was used to account for the influence of solvent (dimethylsulfoxide used). The values given below (NMR data for lyxose) are the difference of the calculated shifts and the shifts of tetramethylsilane computed on the same level of theory.

4.4. Spectroscopy

NMR spectra were recorded at room temperature on Jeol ECP 270 (^1H: 270 MHz, ^{13}C: 67.9 MHz, ^{29}Si: 53.7 MHz), Jeol ECX 400/ECP 400 (^1H: 400 MHz, ^{13}C: 100 MHz, ^{29}Si: 79.4 MHz) and Jeol ECP 500 (^1H: 500 MHz, ^{13}C: 125 MHz, ^{29}Si: 99.4 MHz) spectrometers. The signals of the (deuterated) solvent were used as an internal secondary reference for ^{13}C NMR spectra. ^{29}Si shift values were referenced externally to TMS. NMR signals were assigned by ^1H–^1H COSY45, ^1H–^{13}C HMQC and ^1H–^{13}C HMBC experiments. Shift differences are given as $\delta(C_{complex}) - \delta(C_{free\ sugar})$, the values for the free glycoses were taken from own measurements in DMF or DMSO (D-lyxose). A modified Karplus relationship was used for the interpretation of the coupling constants.[42,43]

To a cooled (0 °C) solution or suspension (lyxose) of the respective glycose (0.023 g, 0.15 mmol) in *N*,*N*-dimethylformamide-d_7 (1 mL) Si(*t*Bu)$_2$(OTf)$_2$ (0.11 mL, 0.33 mmol) was added dropwise. After stirring for 3 h ^1H, ^{13}C, ^{29}Si and 2D NMR spectra were recorded. For all compounds, the ^{13}C NMR signals of the *t*Bu function was found in the ranges 25.5–28.7 ppm (CH_3) and 19.3–22.7 ppm (C_{quart}); the shift range of ^1H NMR signals was 1.32–0.87 ppm.

4.4.1. Arabinose

Si$_2$(*t*Bu)$_4$(β-D-Ara*f*H$_{-4}$-κ*O*^{1,2},κ*O*^{3,5}). ^1H NMR: 5.68 (d, 1H, H1, $^3J_{1,2}$ = 5.1 Hz), 4.47 (dd, 1H, H2, $^3J_{1,2}$ = 5.1 Hz, $^3J_{2,3}$ = 5.3 Hz), 4.25 (dd, 1H, H5a, $^3J_{4,5a}$ = 5.1 Hz, $^2J_{5a,5b}$ = −9.2 Hz), 4.00–3.92 (m, 1H, H3), 3.80 (dd, 1H, H5b, $^3J_{4,5b}$ = 10.4 Hz, $^2J_{5a,5b}$ = −9.2 Hz), 3.60 (ddd, 1H, H4, $^3J_{3,4}$ = 9.5 Hz, $^3J_{4,5a}$ = 5.1 Hz, $^3J_{4,5b}$ = 10.4 Hz). $^{13}C\{^1H\}$ NMR: 101.6 (C1), 83.1 (C3), 83.0 (C2), 72.4 (C4), 67.5 (C5). $^{29}Si\{^1H\}$ NMR: 25.4, −5.5.

Si$_2$(*t*Bu)$_4$(β-D-Ara*p*H$_{-4}$-κ*O*^{1,2},κ*O*^{3,4}). ^1H NMR: 5.42 (d, 1H, H1, $^3J_{1,2}$ = 5.3 Hz), 4.39 (dd, 1H, H3, $^3J_{2,3}$ = 2.1 Hz, $^3J_{3,4}$ = 7.7 Hz), 4.28–4.25 (m, 1H, H4), 4.19 (dd, 1H, H2, $^3J_{1,2}$ = 5.3 Hz, $^3J_{2,3}$ = 2.1 Hz), 3.46 (dd, 1H, H5a, $^3J_{4,5a}$ = 4.5 Hz, $^2J_{5a,5b}$ = −12.77 Hz), 4.03–3.94 (m, 1H, H5b). $^{13}C\{^1H\}$ NMR: 96.3 (C1), 76.5 (C2), 75.7 (C3), 69.6 (C4), 62.4 (C5). $^{29}Si\{^1H\}$ NMR: 16.9, 16.1. Confer the published coupling constants for the bis(phenylborylene) analogue: $J_{1,2}$ 6.0, $J_{2,3}$ 2.4, $J_{3,4}$ 8.6, $J_{4,5a}$ 1.5 Hz.[5]

Si$_2$(*t*Bu)$_4$(D-Ara*a*H$_{-4}$-κ*O*^{2,3},κ*O*^{4,5}). ^1H NMR: 9.70 (d, 1H, H1, $^3J_{1,2}$ = 0.9 Hz), 4.52–4.48 (m, 1H, H2), 4.14–4.10 (m, 1H, H4), 4.10–4.06 (m, 1H, H5a), 3.95–3.89 (m, 1H, H3), 3.76–3.71 (m, 1H, H5b). $^{13}C\{^1H\}$ NMR: 199.3 (C1), 82.5, 78.0, 77.1, 67.9. $^{29}Si\{^1H\}$ NMR: 20.8, 18.3.

4.4.2. Lyxose

Si$_2$(*t*Bu)$_4$(α-D-Lyx*p*H$_{-4}$-κ*O*^{1,4},κ*O*^{2,3}). ^1H NMR: 5.71 (d, 1H, H1, $^3J_{1,2}$ = 2.8 Hz), 4.54 (dd, 1H, H2, $^3J_{1,2}$ = 2.8 Hz, $^3J_{2,3}$ = 5.6 Hz), 4.89 (dd, 1H, H3, $^3J_{2,3}$ = 5.6 Hz, $^3J_{3,4}$ = 7.3 Hz), 4.18–4.14 (m, 2H, H4 and H5a), 3.87–3.84 (m, 1H, H5b). $^{13}C\{^1H\}$ NMR: 102.6 (C1), 79.9 (C2), 75.7 (C4), 74.2 (C3), 64.0 (C5). $^{29}Si\{^1H\}$ NMR: 24.2, −5.6. B3LYP/6-31+G(2d,p)//PBE1PBE/6-311++g(2d,p)-calcd ^{13}C NMR shifts: 99.8 (C1), 79.4 (C2), 75.3 (C4), 74.4 (C3), 66.5 (C5).

Si$_2$(*t*Bu)$_4$(D-Lyx*a*H$_{-4}$-κ*O*^{2,4},κ*O*^{3,5}). ^1H NMR: 9.74 (d, 1H, H1, $^3J_{1,2}$ = 2.2 Hz), 4.67 (dd, 1H, H3, $^3J_{2,3}$ = 9.7 Hz, $^3J_{3,4}$ = 6.2 Hz), 4.33 (dd, 1H, H2, $^3J_{1,2}$ = 2.2 Hz, $^3J_{2,3}$ = 9.7 Hz), 4.35–4.31 (m, 1H, H4), 4.07–3.95 (m, 2H, H5a,b). $^{13}C\{^1H\}$ NMR: 199.4 (C1), 76.2 (C2), 71.2 (C3), 70.4 (C4), 64.0 (C5). $^{29}Si\{^1H\}$ NMR: −5.6, −5.8.

4.4.3. Ribose

Si$_2$(*t*Bu)$_4$(β-D-Rib*f*H$_{-4}$-κ*O*^{2,3},κ*O*^{1,5}). ^1H NMR: 5.49 (s, 1H, H1), 4.53 (d, 1H, H2, $^3J_{2,3}$ = 6.0 Hz), 4.85 (dd, 1H, H3, $^3J_{2,3}$ = 6.0 Hz, $^3J_{3,4}$ = 1.5 Hz), 4.40 (dd, 1H, H4, $^3J_{3,4}$ = 1.5 Hz, $^3J_{4,5a\ or\ 5b}$ = 2.8 Hz), 4.15–4.08 (m, 2H, H5a and H5b). $^{13}C\{^1H\}$ NMR: 106.2 (C1), 91.4 (C4), 86.5 (C2), 81.1 (C3), 68.0 (C5). $^{29}Si\{^1H\}$ NMR: 22.9, −4.4.

Si(*t*Bu)$_2$(β-D-Rib*f*H$_{-2}$-κ*O*^{3,5}). ^1H NMR: 5.81 (d, 1H, H1, $^3J_{1,2}$ = 3.6 Hz), 4.61 (dd, 1H, H2, $^3J_{1,2}$ = 3.6 Hz, $^3J_{2,3}$ = 4.7 Hz), 4.28 (dd, 1H, H4, $^3J_{4,5a}$ = 5.2 Hz, $^3J_{4,5b}$ = 9.3 Hz), 3.94 (dd, 1H, H3, $^3J_{2,3}$ = 4.7 Hz, $^3J_{3,4}$ = 9.3 Hz), 3.75 (dd, 1H, H5b, $^3J_{4,5b}$ = 9.3 Hz, $^2J_{5a,5b}$ = −10.2 Hz). $^{13}C\{^1H\}$ NMR: 103.6 (C1), 78.3 (C3), 77.7 (C2), 73.3 (C4), 67.6 (C5). $^{29}Si\{^1H\}$ NMR: −5.9.

Si$_2$(*t*Bu)$_4$(D-Rib*a*H$_{-4}$-κ*O*^{2,4},κ*O*^{3,5}). ^1H NMR: 9.77 (d, 1H, H1, $^3J_{1,2}$ = 1.4 Hz), 4.40 (dd, 1H, H2, $^3J_{1,2}$ = 1.4 Hz, $^3J_{2,3}$ = 9.3 Hz), 4.01 (t, 1H, H3, $^3J_{2,3}$ = $^3J_{3,4}$ = 9.3 Hz), 4.16–4.12 (m, 1H, H5a), 4.12–4.08 (m, 1H, H4), 3.81–3.76 (m, 1H, H5b). $^{13}C\{^1H\}$ NMR: 199.0 (C1), 81.0 (C2), 74.2 (C3), 72.4 (C4), 68.6 (C5). $^{29}Si\{^1H\}$ NMR: −6.3, −7.0.

4.4.4. Xylose

Si$_2$(*t*Bu)$_4$(α-D-Xyl*f*H$_{-4}$-κ*O*^{1,2},κ*O*^{3,5}). ^1H NMR: 5.94 (d, 1H, H1, $^3J_{1,2}$ = 3.9 Hz), 4.57 (d, 1H, H3, $^3J_{3,4}$ = 2.6 Hz), 4.50 (d, 1H, H2, $^3J_{1,2}$ = 3.9 Hz), 4.39 (dd, 1H, H5a, $^3J_{4,5a}$ = 1.9 Hz, $^2J_{5a,5b}$ = −13.3 Hz), 4.26–4.19 (m, 2H, H4 and H5b). $^{13}C\{^1H\}$ NMR: 103.4 (C1), 87.5 (C2), 79.9 (C3), 77.3 (C4), 63.4 (C5). $^{29}Si\{^1H\}$ NMR: 20.7, −11.0.

Si$_2$(*t*Bu)$_4$(D-Xyl*a*H$_{-4}$-κ*O*^{2,3},κ*O*^{4,5}). ^1H NMR: 9.75 (d, 1H, H1, $^3J_{1,2}$ = 1.5 Hz), 4.47 (dd, 1H, H2, $^3J_{1,2}$ = 1.5 Hz, $^3J_{2,3}$ = 9.2 Hz), 4.18–4.13 (m, 1H, H4), 4.05 (dd, 1H, H5a, $^3J_{4,5a}$ = 5.8 Hz, $^2J_{5a,5b}$ = 8.9 Hz), 4.01 (dd, 1H, H3, $^3J_{2,3}$ = 9.2 Hz, $^3J_{3,4}$ = 2.1 Hz), 3.86 (dd, 1H, H5b, $^3J_{4,5b}$ = 10.3 Hz, $^3J_{5a,5b}$ = −8.9 Hz). $^{13}C\{^1H\}$ NMR: 201.9 (C1), 80.0 (C2), 74.9 (C4), 74.6 (C3), 65.9 (C5). $^{29}Si\{^1H\}$ NMR: 19.7, 17.2.

4.5. Synthesis of crystalline compounds

Si$_2$(*t*Bu)$_4$(D-Lyx*a*H$_{-4}$-κ*O*^{2,4},κ*O*^{3,5}) (**3**). Si(*t*Bu)$_2$(OTf)$_2$ (1.1 mL, 3.3 mmol) was added dropwise to a cooled (0 °C) suspension of D-lyxose (0.23 g, 1.5 mmol) in *N*,*N*-dimethylformamide (10 mL). After stirring for 3 h, colourless rods of **3** precipitated from the dark brown solution. The reaction mixture was allowed to warm up to room temperature and filtered. The precipitate was washed twice with DMF. Yield of a first crystal harvest, not optimised: 47%. Mass spectra: *m*/*z* (DCI$^+$): 431.3 (54%, M+H), 373.2 (11), 74.1 (51), 57.2 (100, *t*Bu), 43.1 (23).

Si$_2$(*t*Bu)$_4$(β-D-Rib*f*H$_{-4}$-κ*O*^{1,5},κ*O*^{2,3}) (**2**): D-ribose (0.23 g, 1.5 mmol) was dissolved in *N*,*N*-dimethylformamide (10 mL) at 0 °C. Right after the dropwise addition of Si(*t*Bu)$_2$(OTf)$_2$ (1.1 mL, 3.3 mmol), a colourless solid began to precipitate from the light yellow solution. After stirring for 3 h the solvent was evaporated by distillation at low temperature and the product was purified by flash chromatography (dichloromethane/methanol; 98:2) to give **2** as colourless crystals. Yield: 62%. Mass spectra: *m*/*z* (DCI$^+$): calcd for $C_{21}H_{43}O_5Si_2$ (M+H): 431.2649, found 431.2650.

Si$_2$(*t*Bu)$_4$(α-*rac*-Xyl*f*H$_{-4}$-κ*O*^{1,2},κ*O*^{3,5}) (*rac*-**1**): Si(*t*Bu)$_2$(OTf)$_2$ (1.1 mL, 3.3 mmol) was added dropwise to a cooled (0 °C) solution of *rac*-xylose (0.23 g, 1.5 mmol) in *N*,*N*-dimethylformamide (10 mL). After stirring for 3 h, the clear yellow solution was allowed to warm up to room temperature. Colourless, solvent-free crystals of *rac*-**1** were obtained after three weeks. Yield of a first crystal harvest, not optimised: 36%. Mass spectra: *m*/*z* (DCI$^+$): 431.3 (3%, M+H), 74.1 (14), 57.2 (100, *t*Bu), 43.1 (21).

Acknowledgement

This work was funded by the Deutsche Forschungsgemeinschaft (Grant Kl 624/11-1).

References

1. Arendt, Y.; Labisch, O.; Klüfers, P. *Carbohydr. Res.* **2009**, *344*, 1213–1224.
2. Connelly, N. G.; Damhus, T.; Hartshorn, R. M.; Hutton, A. T. *Nomenclature of Inorganic Chemistry: IUPAC Recommendations 2005*; The Royal Society of Chemistry: Cambridge, 2005.
3. McNaught, A. D. *Pure Appl. Chem.* **1996**, *68*, 1919–2008.
4. Klüfers, P.; Kunte, T. *Eur. J. Inorg. Chem.* **2002**, 1285–1289.
5. Reichvilser, M. M.; Heinzl, C.; Klüfers, P. *Carbohydr. Res.* **2010**, *345*, 498–502.
6. Ghaschghaie, N.; Hoffmann, T.; Steinborn, M.; Klüfers, P. *Dalton Trans.* **2010**, *39*, 5535–5543.
7. Allscher, T.; Klüfers, P. *Carbohydr. Res.* **2009**, *344*, 539–540.
8. Taylor, G. E.; Waters, J. M. *Tetrahedron Lett.* **1981**, *22*, 1277–1278.
9. Drew, K. N.; Zajicek, J.; Bondo, G.; Bose, B.; Serianni, A. S. *Carbohydr. Res.* **1998**, *307*, 199–209.
10. Kim, K.; Kim, H.-J.; Oh, D.-K.; Cha, S.-S.; Rhee, S. *J. Mol. Biol.* **2006**, *361*, 920–931.
11. Yoshida, H.; Yamada, M.; Ohyama, Y.; Takada, G.; Izumori, K.; Kamitori, S. *J. Mol. Biol.* **2007**, *365*, 1505–1516.
12. Yoshida, H.; Yamada, M.; Nishitani, T.; Takada, G.; Izumori, K.; Kamitori, S. *J. Mol. Biol.* **2007**, *374*, 443–453.
13. Kovalevsky, A. Y.; Katz, A. K.; Carrell, H. L.; Hanson, L.; Mustyakimov, M.; Fisher, S. Z.; Coates, L.; Schoenborn, B. P.; Bunick, G. J.; Glusker, J. P.; Langan, P. *Biochemistry* **2008**, *47*, 7595–7597.
14. Yoshida, H.; Yamaji, M.; Ishii, T.; Izumori, K.; Kamitori, S. *FEBS J.* **2010**, *277*, 1045–1057.
15. Betz, R.; Klüfers, P. *Inorg. Chem.* **2009**, *48*, 925–935.
16. Corey, E. J.; Hopkins, P. B. *Tetrahedron Lett.* **1982**, *23*, 4871–4874.
17. Furusawa, K.; Ueno, K.; Katsura, T. *Chem. Lett.* **1990**, *19*, 97–100.
18. Ueno, K.; Furusawa, K.; Katsura, T. *Acta Crystallogr., Sect. C* **1990**, *46*, 1509–1513.
19. Serebryany, V.; Beigelman, L. *Tetrahedron Lett.* **2002**, *43*, 1983–1985.
20. Plet, J. R. H.; Porter, M. J. *Chem. Commun.* **2006**, 1197–1199.
21. Zhu, X.; Kawatkar, S.; Rao, Y.; Boons, G.-J. *J. Am. Chem. Soc.* **2006**, *128*, 11948–11957.
22. Nacario, R. C.; Lowary, T. L.; McDonald, R. *Acta Crystallogr., Sect. E* **2007**, *63*, o498–o500.
23. Imamura, A.; Ando, H.; Ishida, H.; Kiso, M. *Curr. Org. Chem.* **2008**, *12*, 675–689.
24. Mortimer, A. J. P.; Aliev, A. E.; Tocher, D. A.; Porter, M. J. *Org. Lett.* **2008**, *10*, 5477–5480.
25. Wang, Y.; Maguire-Boyle, S.; Dere, R. T.; Zhu, X. *Carbohydr. Res.* **2008**, *343*, 3100–3106.
26. Ali, A.; van den Berg, R. J. B. H. N.; Overkleeft, H. S.; Filippov, D. V.; van der Marel, G. A.; Codée, J. D. C. *Tetrahedron Lett.* **2009**, *50*, 2185–2188.
27. Koizumi, A.; Hada, N.; Kaburaki, A.; Yamano, K.; Schweizer, F.; Takeda, T. *Carbohydr. Res.* **2009**, *344*, 856–868.
28. Haraguchi, K.; Konno, K.; Yamada, K.; Kitagawa, Y.; Nakamura, K. T.; Tanaka, H. *Tetrahedron* **2010**, *66*, 4587–4600.
29. Dworkin, J. P.; Miller, S. L. *Carbohydr. Res.* **2000**, *329*, 359–365.
30. Hayward, D. L.; Angyal, S. J. *Carbohydr. Res.* **1977**, *53*, 13–20.
31. Wu, J.; Serianni, A. S.; Vuorinen, T. *Carbohydr. Res.* **1990**, *206*, 1–12.
32. Vuorinen, T.; Serianni, A. S. *Carbohydr. Res.* **1991**, *209*, 13–31.
33. Funcke, W.; von Sonntag, C.; Triantaphylides, C. *Carbohydr. Res.* **1979**, *75*, 305–309.
34. Yaylayan, V. A.; Ismail, A. A. *J. Carbohydr. Chem.* **1992**, *11*, 149–158.
35. Zhu, Y.; Zajicek, J.; Serianni, A. S. *J. Org. Chem.* **2001**, *66*, 6244–6251.
36. Lewis, B. E.; Choytun, N.; Schramm, V. L.; Bennet, A. J. *J. Am. Chem. Soc.* **2006**, *128*, 5049–5058.
37. Silva, A. M.; da Silva, E. C.; da Silva, C. O. *Carbohydr. Res.* **2006**, *341*, 1029–1040.
38. Eitelman, S. J.; Horton, D. *Carbohydr. Res.* **2006**, *341*, 2658–2668.
39. Mossine, V. V.; Barnes, C. L.; Chance, D. L.; Mawhinney, T. P. *Angew. Chem., Int. Ed.* **2009**, *48*, 5517–5520.
40. Klüfers, P.; Kopp, F.; Vogt, M. *Chem. Eur. J.* **2004**, *10*, 4538–4545.
41. Frisch, M. J.; Trucks, G. W.; Schlegel, H. B.; Scuseria, G. E.; Robb, M. A.; Cheeseman, J. R.; Montgomery, J. A.; Vreven, T.; Kudin, K. N.; Burant, J. C.; Millam, J. M.; Iyengar, S. S.; Tomasi, J.; Barone, V.; Mennucci, B.; Cossi, M.; Scalmani, G.; Rega, N.; Petersson, G. A.; Nakatsuji, H.; Hada, M.; Ehara, M.; Toyota, K.; Fukuda, R.; Hasegawa, J.; Ishida, M.; Nakajima, T.; Honda, Y.; Kitao, O.; Nakai, H.; Klene, M.; Li, X.; Knox, J. E.; Hratchian, H. P.; Cross, J. B.; Bakken, V.; Adamo, C.; Jaramillo, J.; Gomperts, R.; Stratmann, R. E.; Yazyev, O.; Austin, A. J.; Cammi, R.; Pomelli, C.; Ochterski, J. W.; Ayala, P. Y.; Morokuma, K.; Voth, G. A.; Salvador, P.; Dannenberg, J. J.; Zakrzewski, V. G.; Dapprich, S.; Daniels, A. D.; Strain, M. C.; Farkas, O.; Malick, D. K.; Rabuck, A. D.; Raghavachari, K.; Foresman, J. B.; Ortiz, J. V.; Cui, Q.; Baboul, A. G.; Clifford, S.; Cioslowski, J.; Stefanov, B. B.; Liu, G.; Liashenko, A.; Piskorz, P.; Komaromi, I.; Martin, R. L.; Fox, D. J.; Keith, T.; Laham, A.; Peng, C. Y.; Nanayakkara, A.; Challacombe, M.; Gill, P. M. W.; Johnson, B.; Chen, W.; Wong, M. W.; Gonzalez, C.; Pople, J. A. Gaussian, Inc.: Wallingford, 2004.
42. Haasnoot, C. A. G.; de Leeuw, F. A. A. M.; Altona, C. *Tetrahedron* **1980**, *36*, 2783–2792.
43. Navarro-Vazquez, A.; Cobas, J. C.; Sardina, F. J.; Casanueva, J.; Diez, E. *J. Chem. Inf. Comput. Sci.* **2004**, *44*, 1680–1685.